HHS Public Access

Author manuscript

J Bone Miner Res. Author manuscript; available in PMC 2019 July 18.

Published in final edited form as:

J Bone Miner Res. 2019 March ; 34(3): 482–489. doi:10.1002/jbmr.3628.

A Heterozygous Splice-Site Mutation in *PTHLH* Causes Autosomal Dominant Shortening of Metacarpals and Metatarsals

Monica Reyes[1], **Bert Bravenboer**[2], and **Harald Jüppner**[1,3]

[1]Endocrine Unit, Massachusetts General Hospital and Harvard Medical School, Boston, MA, USA

[2]Department of Endocrinology, Universitair Ziekenhuis Brussels, Brussels, Belgium

[3]Pediatric Nephrology Unit, Massachusetts General Hospital and Harvard Medical School, Boston, MA, USA

Abstract

Short metacarpals and/or metatarsals are typically observed in pseudohypoparathyroidism (PHP) type la (PHP1A) or pseudo-PHP (PPHP), disorders caused by inactivating *GNAS* mutations involving exons encoding the alpha-subunit of the stimulatory G protein (Gsα). Skeletal abnormalities similar to those in PHP1A/PPHP were present in several members of an extended Belgian family without evidence for abnormal calcium and phosphate regulation. Direct nucleotide sequencing of genomic DNA from an affected individual (190/III-1) excluded *GNAS* mutations. Instead, whole exome analysis revealed a novel heterozygous A>G change at nucleotide —3 upstream of *PTHLH* exon 3 that encodes the last two amino acids of the prosequence and the mature PTHrP. The same nucleotide change was also found in her affected mother and maternal aunt (190/II-2,190/II-1), and her affected twin sons (190/IV-1, 190/IV-2), but not in her unaffected daughter (190/IV-3) and sister (190/III-2). Complementary DNA derived from immortalized lymphoblastoid cells from 190/IV-2 (affected) and 190/IV-3 (unaffected) was PCR-amplified using forward primers located either in *PTHLH* exon 1 (noncoding) or exon 2 (presequence and most of the prosequence), and reverse primers located in the 3'-noncoding regions of exons 3 or 4. Nucleotide sequence analysis of these amplicons revealed for the affected son 190/IV-2, but not for the unaffected daughter 190/IV-3, a heterozygous insertion of genomic nucleotides —2 and —1 causing a frameshift after residue 34 of the pre/prosequence and thus 29 novel residues without homology to PTHrP or any other protein. Our findings extend previous reports indicating that PTHrP haploinsufficiency causes skeletal abnormalities similar to those observed with heterozygous *GNAS* mutations.

Keywords

PTHLH; PARATHYROID HORMONE-RELATED PEPTIDE; GROWTH PLATE; CHONDROCYTES; METACARPALS; METATARSALS

Address correspondence to: Harald Jüppner, MD, Endocrine Unit, Thier 10, Massachusetts General Hospital, Boston, MA., hjueppner@partners.org.

Additional Supporting Information may be found in the online version of this article.

Disclosures

All authors state that they have no conflicts of interest.

Introduction

Shortening of metacarpals and/or metatarsals, namely brachydactyly E (BDE), particularly of the fourth digits, is typically observed in patients affected by pseudohypoparathyroidism (PHP) type la (PHP1A) and pseudo-PHP (PPHP),[1–5] and similar skeletal abnormalities can be encountered, albeit less frequently, in patients affected by PHP type Ib (PHP1B).[6–9] All three PHP variants are caused by genetic or epigenetic abnormalities involving *GNAS* that reduce or abolish generation of the α-subunit of the stimulatory G protein (Gsα) from one parental allele. [3–5,10,11] Importantly, patients affected by PHP1A and PHP1B, but not those affected by PPHP, develop resistance to different hormones that mediate their actions through Gsα-coupled receptors, including resistance to parathyroid hormone (PTH) and thyroid-stimulating hormone (TSH).[2–5,12] The resulting biochemical changes—in particular often profound PTH elevations, hypocalcemia, and hyperphosphatemia—can thus help distinguishing between different genetic defects that are associated with shortened metacarpals and metatarsals. For example, heterozygous mutations affecting phosphodiesterase 4D (*PDE4D*) or the regulatory subunit of protein kinase A (PKA; *PRKAR1A*) lead to acrodysostosis and short stature, often in association with mild hormonal resistance.[13–20] Similar skeletal findings are encountered in patients with mutations in *PDE3A*,[21,22] *SHOX*,[23] or *HDAC4*[24] that are associated with different additional abnormalities. Likewise, mutations in *PTHLH*, the gene encoding PTHrP, lead to shortening of bones in hands and feet, and are usually associated with short stature, but no other clinically apparent defects.[25–31] Importantly, genetic mutations in *GNAS* and *PRKAR1A* (and occasionally in *PDE4D*) are associated with readily detectable laboratory abnormalities. Consequently, the absence or presence of hormonal resistance can help reduce the list of plausible candidate genes that are responsible for shortening of one or several metacarpals.

We investigated a family in which several members presented with skeletal abnormalities involving one or several metacarpals and metatarsals, who showed no biochemical abnormalities. Whole exome sequencing led to the discovery of an intronic *PTHLH* mutation that introduces a novel splice acceptor site resulting in the synthesis of a mutant PTHrP comprising only the peptide's presequence and portions of the prosequence, followed by amino acid residues without homology to PTHrP or another protein in public databases.

Patients and Methods

Patients

Several members in family 190 were evaluated because of clinically apparent shortening of one or several metacarpals without obvious abnormalities in calcium and phosphate homeostasis (Fig. 1A).The first two investigated family members, the females 190/II-1 and 190/III-1, were referred at about the same time for assessment.

The 47-year-old woman, 190/III-1, showed shortening of the third and/or the fourth metacarpals; her height was below the 50th percentile, but well within the normal range (Fig. 1B). She revealed no laboratory abnormalities, which, combined with her radiographic

findings, suggested that she might be affected by PPHP. This raised the concern that her children, her identical twin sons, 190/IV-1 and 190/IV-2 (age: 18 years), or her daughter, 190/IV-3 (age: 19 years), could be affected by PHP1A. However, just the twins revealed shortening only of the fourth metacarpals, whereas the daughter showed no evidence of skeletal abnormalities; all three showed no evidence for PTH-resistant hypocalcemia.

The 84-year-old maternal aunt, 190/II-1, has short hands and feet, clinically apparent shortening of both fourth metacarpals, short stature, a short neck, and obesity, as well as significant rheumatoid arthritis, coronary heart disease, atrial fibrillation, and diabetes mellitus type 2, but no history of recurrent cramps or seizures. Hand radiographs of 190/II-1, which became available after the initial consultation, showed shortening of multiple metatarsals and metatarsals, as well as degenerative changes (Fig. 1C).

Methods

All biochemical measurements, nucleotide sequence analysis of the *GNAS* exons 2 to 13 and portions of exon 1, as well as the search for abnormal *GNAS* methylation was performed at the Universitair Ziekenhuis Brussels, Department of Genetics, Brussels, Belgium.

Whole exome sequencing was performed on 190/II-1 at the Broad Institute in Cambridge, Massachusetts, as previously described[32]; Seqr was used to search for potentially disease-causing variants.

Primers a and d (Supplementary Table 1) were used for amplification of a 985-bp PCR product from genomic DNA that includes the nucleotide change at position −3 upstream of exon 3, as well as SNP rs6253 (Supplementary Fig. 1). PCR was performed with QIAGEN Taq DNA polymerase (QIAGEN, Valencia, CA, USA) following the manufacturer's protocols; cycler program: denaturation at 95°C for 5 min followed by 40 cycles at 95°C for 30 s, 58°C for 30 s, and 72°C for 1 min, followed by an additional elongation step at 72°C for 10 min. Amplicons were purified using ExoSap-IT (Affymetrix, Santa Clara, CA, USA) and sequenced at the DNA core facility of the Massachusetts General Hospital in Boston, Massachusetts.

Lymphoblastoid cells were generated from family members 190/IV-2 (affected) and 190/IV-3 (unaffected) at the Center of Genetic and Genomic Research, Massachusetts General Hospital; cells were immortalized and maintained as previously described.[33] Total RNA was isolated using TRIZol (ThermoFisher, Waltham, MA, USA) followed by silica column purification according to the manufacturer's instructions (Ambion Pure Link; Invitrogen, Waltham, MA, USA). TAKARA PrimeScript RT reagent kit with gDNA eraser (Cat. #RR047A; TAKARA, Shiga, Japan) were used for reverse transcription of 1 mg of total RNA according to the manufacturer's instructions. RT-PCR was performed using forward and reverse primers listed in Supplementary Table 1: cycler program: denaturation at 95°C for 5min followed by 40 cycles at 95°C for 30 s, at 58°C for 30 s, and at 72°C for 1 min, followed by an additional elongation step at 72°C for 10 min.

To determine whether the eventually identified genomic nucleotide change causes abnormal splicing that is readily detectable by agarose gel electrophoresis or leads to a 2-bp insertion, as predicted based on the introduction of a putative novel splice acceptor site, cDNA from the affected son, 190/IV-2 and the unaffected daughter, 190/IV-3 was amplified using the reverse primer d, in combination with forward primers e, f, or g (Supplementary Fig. 2 and Supplementary Table 1); each of these amplicons includes the region comprising the putative insertion as well as SNP rs6253. When combining reverse primer d with forward primer c, a 443-bp amplicon derived from the 3'-noncoding region was amplified that contains rs6253, but not the insertion. The PCR products from both individuals were sequenced directly using forward primer h, and the amplicons obtained with primers f and d, and with primers e and d, were furthermore cloned using TOPO TA cloning kit and one shote T0P010 chemically competent *E. coli* (catalog #K4500-J10; pCR 2.1-TOPO vector 3.9 kb; ThermoFisher). Plasmid DNA derived from several independent bacterial colonies was sequenced using vector-specific forward and reverse primers to assess the presence or absence of the 2-bp AG insertion combined with either 'a' or 'g' at rs6253.

Genetic analyses were performed after obtaining informed consent from the investigated family members using forms approved by the institutional review board of Massachusetts General Hospital.

Results

Clinical and laboratory findings

The two oldest members in family 190, the affected mother, 190/II-2 and her affected sister, 190/II-1, revealed shortening of multiple metacarpals and metatarsals as well as short stature. The deceased mother of these two patients reportedly had similar findings, as did three of that mother's 10 siblings, who are also deceased; it is unknown whether any of these three presumably affected individuals have descendants with similar clinical findings. In contrast to the broader skeletal abnormalities in patients 190/II-1 and 190/II-2, the affected members in the next generation showed only shortening of the third and/or fourth metacarpals. The disorder thus follows an autosomal dominant trait with complete penetrance, but variable severity. Note that the genetic defect underlying the skeletal abnormalities had been transmitted by two females. However, the affected daughter of 190/II-2, namely 190/III-1, and the affected twin sons of 190/III-1, namely 190/IV-1 and 190/IV-2, have normal levels for calcium, phosphate, PTH, and TSH (see Fig. 1).

Identification of the genetic defect in *PTHLH*

Shortening of the fourth metacarpals can be found in patients affected by either PHP1A or PPHP.[3–5] *GNAS* exons 2 to 13 and exon 1 codons 13 to 40 were therefore sequenced when 190/III-1 was first evaluated. However, no evidence for a disease-causing mutation was identified, and there was no evidence for *GNAS* methylation changes (data not shown). Genomic DNA of the maternal aunt 190/II-1 was therefore submitted for whole exome sequencing, which revealed 3315 heterozygous variants with an allele frequency of less than 0.01, 137 of which were nonsense or essential splice site mutations, or indels leading to frameshift changes. No evidence for a mutation in coding or noncoding exons was identified

in candidate genes, including *GNAS* (thus confirming the earlier negative direct sequence analyses; see above), *PDE4D*, *PDE3A*, *HDAC4*, *SHOX*, *PRKAR1A* and *PTHLH*.

However, a heterozygous variant was observed at position −3 upstream of *PTHLH* exon 3 (Fig. 2A), which transitions adenine to guanine (a>g). This nucleotide change was predicted to generate a novel splice acceptor site two nucleotides further upstream, namely 'cag' at positions −5, −4, and −3 instead of 'aag' at positions −3, −2, and −1. The genomic a>g change, which is not found in public databases, was confirmed by direct nucleotide sequence analysis of genomic DNA (Fig. 2B). Search for this nucleotide change in all available family members revealed 'a/g' heterozygosity at the splice acceptor site for the five affected, but 'a' homozygosity for the two unaffected family members (Supplementary Fig. 1). These findings made it likely that the identified genomic 'g' variant in *PTHLH* is responsible for the skeletal abnormalities encountered in the affected members of family 190.

The novel splice site variant leads to a mutant mRNA and causes PTHrP haploinsufficiency

To explore whether the nucleotide variant at position −3 upstream of exon 3 causes abnormal splicing of the *PTHLH* pre-mRNA, total RNA was extracted from immortalized lymphoblastoid cells that had been established for the affected male 190/IV-2 and his unaffected sister 190/IV-3. After reverse transcription, cDNAs from both family members were amplified using different forward primers located in exons 1 and 2, respectively, in combination with a reverse primer located in the 3' noncoding region downstream of exon 3; cDNAs from both siblings were also amplified using a forward primer in exon 2 and a reverse primer located 3' of exon 4 (Fig. 3A, Supplementary Fig. 2A, and Supplementary Table 1). For individuals 190/IV-2 and 190/IV-3, these experiments led to five readily detectable primary amplicons (Supplementary Fig. 2B,C) that were of the expected sizes indicating that lymphoblastoid cells express the mRNAs giving rise to the splice variants PTHrP(1–139) and PTHrP(1–141), and that the a>g transition at the splice acceptor site upstream of exon 3 did not lead to the generation of splice variants that are significantly different from the sizes of the amplicons derived from the wild-type allele.

Nucleotide sequence analysis of the DNA bands derived from the unaffected daughter 190/IV-3, encoding PTHrP(1–139) and PTHrP(1–141), revealed only wild-type *PTHLH* sequences when using the forward sequencing primer *h* (Fig. 3B, upper sequences). The corresponding amplicons derived from the affected son 190/IV-2 provided wild-type *PTHLH* sequence up to codon −3 of proPTHrP, which was followed by two overlapping nucleotide sequences (Fig. 3B, lower sequences). Further analysis of these double sequences revealed the wild-type cDNA and a second sequence comprising an insertion of two base pairs, A and G, that are derived from genomic DNA at positions-2 and −1 just upstream of exon 3. Because of these two additional nucleotides in the mutant cDNA, a frameshift is introduced, thus changing the open-reading frame after codon −3. As a result, the entire prePTHrP sequence and the first four amino acid residues of the proPTHrP sequence are translated normally, followed by 29 residues that are unrelated to PTHrP and share no homology with other proteins in available databases (Fig. 3C); no functional PTHrP is therefore generated from the mutant *PTHLH* allele. The skeletal phenotype of the affected

family members is thus likely caused by the point mutation at the splice acceptor site of exon 3 and the resulting PTHrP haploinsufficiency.

Patient 190/IV-2 inherited the mutant PTHLH allele from his affected mother

To confirm that the mutant mRNA with the 2-bp insertion is derived in the affected individual 190/IV-2 from the maternal *PTHLH* allele, we took advantage of SNP rs6253 that is heterozygous ‘a/g’ in the twins 190/IV-1 and 190/IV-2, yet homozygous ‘a’ in the maternal aunt 190/II-1, the affected mother 190/II-2, the patient 190/III-1, and the unaffected daughter 190/IV-3 (Supplementary Fig. 3). This predicted that the disease-causing genomic ‘g’ variant at the splice acceptor site upstream of *PTHLH* exon 3 is associated with ‘a’ at rs6253. Note that the unaffected father of the three siblings in the fourth generation (see Fig. 1), who was not available for testing, has to be heterozygous ‘a/g’ for rs6253. Complementary DNA clones derived from the mutant maternal *PTHLH* allele of 190/IV-2 would therefore be predicted to comprise the AG’ insertion as well as a’ for SNP rs6253, whereas clones derived from the paternal wild-type *PTHLH* allele would have no insertion and ‘g’ at the nucleotide polymorphism.

PCR amplicons using primers f and d (see Supplementary Fig. 2B) were cloned and sequence analysis was informative for plasmid DNAs derived from 18 independent bacterial colonies. Seven clones from affected son 190/IV-2 had the ‘AG’ insertion in combination with ‘a’ at rs6253, whereas 11 clones without the insertion were ‘g’ at the SNP. Similar results were obtained when cloning the PCR product obtained with primers e and d (data not shown). These experiments showed that the mutant mRNA derived from lymphoblastoid cells of patient 190/IV-2 is transcribed from the maternal *PTHLH* allele.

Discussion

Shortening of the fourth metacarpals and metatarsals, with or without shortening of additional bones in the hands and feet can be caused by heterozygous mutations in several different genes. The gender of the parent transmitting these skeletal findings, and the absence or presence of additional clinical and/or laboratory abnormalities may allow predictions regarding the underlying genetic defect. For example, *PDE3A* mutations can cause skeletal changes that are associated with hypertension without mineral ion abnormalities,[21,22] whereas some *PDE4D* mutations and the known *PRKAR1A* mutations can lead to mild hormonal resistance, as evidenced by slightly elevated PTHand/orTSH levels.[13–20]The heterozygous mutations identified in these three genes appear to either accelerate cAMP metabolism (*PDE* mutations) or limit, through dominant-negative mechanisms, PKA activation (*PRKAR1A* mutations). Likewise, heterozygous HDAC4 mutations limit signaling events downstream of PKA and are thereby responsible for accelerated bone maturation, as well as other features, including mental retardation and obesity.[24,34] Reduced intracellular cAMP levels or limited resistance to this second messenger thus appear to be sufficient for accelerating chondrocyte differentiation and premature growth plate closure, particularly at the fourth metacarpals and metatarsals that seem to be particularly sensitive to locally reduced levels of this second messenger.

Skeletal findings that are indistinguishable from those caused by heterozygous mutations in the above genes can also be due to heterozygous inactivating mutations involving *GNAS* exons 1 to 13, or by methylation changes at this complex genetic locus.[3–9] These genetic or epigenetic defects are the cause of PHP1A and PHP1B, respectively, if they involve the maternal allele, and thus lead to PTH-resistant hypocalcemia and hyperphosphatemia. Further-more, TSH is frequently elevated; particularly PHP1A patients present with additional abnormalities, such as early-onset obesity, short stature, and various degrees of neurodevelopmental challenges, findings that are referred to as Albright hereditary osteodystrophy (AHO). The same or similar mutations on the paternal allele lead to PPHP, ie, AHO without hormonal resistance and without obesity or neurocognitive abnormalities.[2–5,10,11,35–37]

Likewise, PTHrP haploinsufficiency can lead to variable shortening of one or multiple metacarpals and metatarsals, but also to short stature implying that chondrocytes in multiple growth plates undergo accelerated differentiation.[25–31] It is therefore likely that haploinsufficiency of PTHrP-dependent signaling at the PTHR1 reduces intracellular cAMP levels in growth plate chondrocytes to a similar extent as heterozygous *PDE4D*, *PDE3A*, and *PRKAR1A* mutations, or the reduction of Gsα protein levels through genetic or epigenetic mechanisms.

When the female patient 190/III-1 was first referred for evaluation of shortened metacarpals and metatarsals, serum calcium and phosphate levels were shown to be within normal limits, which raised the concern that she might be affected by PPHP and that some of her children could be affected by PHP1A. However, analysis of *GNAS* provided no evidence for a genetic or epigenetic abnormality. Consistent with a lack of *GNAS* abnormalities affecting Gsα function or expression, her affected twin boys revealed normal calcium, PTH, and TSH levels, thus making a PHP variant unlikely, despite the maternally inherited skeletal phenotype (see Fig. 1).

Whole exome sequencing subsequently revealed a heterozygous adenine-to-guanine exchange at position −3 upstream of *PTHLH* exon 3. This variant was identified in the five affected, but not in the two available unaffected family members, and thus appeared to be genetically linked to the skeletal phenotype. The identified nucleotide exchange was predicted to generate a novel splice acceptor site, which predicted that exon 3 would be extended at the 5’ end by two additional nucleotides (A and G) and that the mRNA transcribed from the mutant *PTHLH* gene would therefore carry a 2-bp insertion.

Previous reports describing the use of peripheral white blood cells for total RNA extraction had failed to detect *PTHLH* transcripts by RT-PCR; however, details regarding the forward and reverse primers, and the conditions for PCR amplification had not been provided in these earlier studies.[28,29] To determine whether immortalized lymphoblastoid cells would allow PCR amplification of the mRNA encoding PTHrP, we generated such cells from an affected and an unaffected member of family 190. After optimization, the two major PTHrP splice variants, PTHrP(1–139) and PTHrP(1–141), could be amplified across introns as primary PCRs with several different combinations of forward primers and reverse primers. These studies showed that cDNAs encoding both PTHrP variants can be readily amplified

from lymphoblastoid cells and that the amplicons derived from the affected and the unaffected family member are of the expected sizes, thus excluding major abnormalities in pre-mRNA processing.

However, the amplicons encoding PTHrP(1–139) and PTHrP (1–141) that were derived from the affected son 190/IV-2, but not those derived from his unaffected sister 190/IV-3, revealed a heterozygous 2-bp insertion of the genomic nucleotides located at positions −2 and −1 upstream of *PTHLH* exon 3. These findings confirmed that the genomic adenine-to-guanine change upstream of exon 3 generates a novel splice acceptor site, and that the resulting introduction of two additional nucleotides into the mRNA causes a shift in the open-reading frame after codon −3 of the prosequence. After synthesis of the presequence and 4 amino acid residues of the prosequence, 29 residues are added that are unrelated to PTHrP and share no homology with other proteins. Cloning of PCR amplicons generated with primers g and d (or with e and d) subsequently revealed that the 2-bp insertion is present in the cDNA derived from the *PTHLH* allele that comprises the ‘a’ nucleotide for SNP rs6253, thus confirming that the affected son 190/IV-2 had inherited the mutant *PTHLH* allele from his mother. Taken together, our data showed that the genomic mutation at the splice acceptor site upstream of *PTHLH* exon 3 leads to abnormal pre-mRNA processing and no functional PTHrP.

Our findings, which are similar to those previously reported by others,[25–29,31] indicate that PTHrP haploinsufficiency causes an acceleration of chondrocyte differentiation leading to premature epiphyseal closure, which appears to be restricted in the younger generations of our kindred to the fourth metacarpals and metatarsals. Comparable skeletal findings are also associated with Gsα haploinsufficiency, as observed in patients affected by PHP1A and PPHP,[2–5] and in several patients affected by PHP1B.[6–9] This suggests that these bones in the hands and feet are uniquely sensitive to decreased expression of PTHrP—the peptide that is required for slowing the hypertrophic differentiation of growth plate chondrocytes.[38] However, the skeletal abnormalities observed in the presented kindred are quite variable, leading to limited skeletal abnormalities in the younger family members with the *PTHLH* mutation, whereas the older affected individuals revealed more extensive abnormalities. Similarly, skeletal findings caused by inactivating Gsα mutations can be variable, ranging from the shortening of only one metacarpal to abnormalities that are indistinguishable from those encountered in acrodysostosis.[2,39] This makes it plausible that genetic modifiers and/or nutritional and environmental factors can affect the severity of the skeletal findings caused by mutations in *GNAS*, *PTHLH*, *PDE4D*, *PDE3A*, *PRKAR1A*, or potentially other genes.

The adult heights of the affected family members younger than 50 years were within the normal range. In fact, based on gender-specific, population-based normative data (Center for Disease Control; https://www.cdc.gov/growthcharts/cdc), the affected individuals 190/III-1, 190/IV-1, and 190/IV-2 had adult height Z-scores of —0.5 to —0.9. This could indicate that the identified *PTHLH* mutation has only a limited impact on chondrocytes in growth plates other than those of a few metacarpals and metatarsals, but does not lead to overtly short stature.

Our findings indicate that haploinsufficiency caused by the heterozygous 2-bp insertion is likely to affect PTHrP(1–139) and PTHrP(1–141). Only one *PTHLH* mutation affects exclusively the PTHrP(1–141) splice variant, namely the c.532A>G; p. (* 178Wext*53) change that was identified in three affected members across three generations (family 4 in reference 25); all other BDE-causing *PTHLH* mutations are predicted to affect PTHrP(1–139) as well as PTHrP(1–141).[25–29,31] It is therefore plausible that PTHrP(1–141), rather than PTHrP(1–139), is required for preventing the premature closure ofgrowth plates, particularly of the fourth metacarpals.

In summary, a novel splice acceptor site mutation in *PTHLH* leads to the generation of an mRNA comprising a 2-bp insertion, which causes a shift in the open-reading frame, thus encoding a mutant PTHLH-derived peptide that comprises most residues of the PreProPTHrP sequence, followed by novel amino acid residues that are unrelated to PTHrP, thus leading to a lack of PTHrP from the mutant *PTHLH* allele. Our findings extend previous reports indicating that PTHrP haploinsufficiency can cause shortening of metacarpals and metatarsals, skeletal findings that are indistinguishable from those observed with mutations in *GNAS* or other genes.

Supplementary Material

Refer to Web version on PubMed Central for supplementary material.

Acknowledgments

This work was supported by NIH grants RO1-DK46718 and PO1 DK11794 (subproject IV) (HJ). We thank the participating family members.

References

1. Albright F, Burnett CH, Smith PH, Parson W. Pseudohypoparathyroidism - an example of “Seabright-Bantam syndrome.” Endocrinology. 1942;30:922–32.
2. Levine MA. Pseudohypoparathyroidism In: Bilezikian JP, Raisz LG, Rodan GA, editors. Principles of bone biology. New York: Academic Press; 2002 p. 1137–59.
3. Weinstein LS, Liu J, Sakamoto A, Xie T, Chen M. Minireview: GNAS: normal and abnormal functions. Endocrinology. 2004;145(12):5459–64. [PubMed: 15331575]
4. Bastepe M, Jüppner H. Pseudohypoparathyroidism, Albright’s hereditary osteodystrophy, and progressive osseous heteroplasia: disorders caused by inactivating GNAS mutations In DeGroot LJ, Jameson JL, editors. Endocrinology. Philadelphia, PA: WB Saunders; 2016 p. 1147–59.
5. Tafaj O, Jüppner H. Pseudohypoparathyroidism: one gene, several syndromes. J Endocrinol Invest. 2017;40:347–56. [PubMed: 27995443]
6. Unluturk U, Harmanci A, Babaoglu M, et al. Molecular diagnosis and clinical characterization of pseudohypoparathyroidism type-Ib in a patient with mild Albright’s hereditary osteodystrophy-like features, epileptic seizures, and defective renal handling of uric acid. Am J Med Sci. 2008;336:84–90. [PubMed: 18626245]
7. Mantovani G, de Sanctis L, Barbieri AM, et al. Pseudohypoparathyroidism and GNAS epigenetic defects: clinical evaluation of Albright hereditary osteodystrophy and molecular analysis in 40 patients. J Clin Endocrinol Metab. 2010;95:651–58. [PubMed: 20061437]
8. Sanchez J, Perera E, Jan de Beur S, et al. Madelung-like deformity in pseudohypoparathyroidism type 1b. J Clin Endocrinol Metab. 2011;96:E1507–11. [PubMed: 21752878]
9. Sharma A, Phillips AJ, Jüppner H. Hypoplastic metatarsals—beyond cosmesis. N Engl J Med. 2015;373:2189–90. [PubMed: 26605941]

10. Patten JL, Johns DR, Valle D, et al. Mutation in the gene encoding the stimulatory G protein of adenylate cyclase in Albright's hereditary osteodystrophy. New Engl J Med. 1990;322:1412–19. [PubMed: 2109828]
11. Weinstein LS, Gejman PV, Friedman E, et al. Mutations of the Gs a-subunit gene in Albright hereditary osteodystrophy detected by denaturing gradient gel electrophoresis. Proc Natl Acad Sci USA. 1990;87:8287–90. [PubMed: 2122458]
12. Usardi A, Mamoune A, Nattes E, Carel JC, Rothenbuhler A, Linglart A. Progressive development of PTH resistance in patients with inactivating mutations on the maternal allele of GNAS. J Clin Endocrinol Metab. 2017;102:1844–50. [PubMed: 28323910]
13. Linglart A, Menguy C, Couvineau A, et al. Recurrent PRKAR1A mutation in acrodysostosis with hormone resistance. N Engl J Med. 2011;364:2218–26. [PubMed: 21651393]
14. Michot C, Le Goff C, Goldenberg A, et al. Exome sequencing identifies PDE4D mutations as another cause of acrodysostosis. Am J Hum Genet. 2012;90:740–45. [PubMed: 22464250]
15. Lee H, Graham JM Jr, Rimoin DL, et al. Exome sequencing identifies PDE4D mutations in acrodysostosis. Am J Hum Genet. 2012;90: 746–51. [PubMed: 22464252]
16. Linglart A, Fryssira H, Hiort O, et al. PRKAR1A and PDE4D mutations cause acrodysostosis but two distinct syndromes with or without GPCR-signaling hormone resistance. J Clin Endocrinol Metab. 2012;97:E2328–38. [PubMed: 23043190]
17. Lynch DC, Dyment DA, Huang L, et al. Identification of novel mutations confirms PDE4D as a major gene causing acrodysostosis. Hum Mutat. 2013;34:97–102. [PubMed: 23033274]
18. Lindstrand A, Grigelioniene G, Nilsson D, et al. Different mutations in PDE4D associated with developmental disorders with mirror phenotypes. J Med Genet. 2014;51:45–54. [PubMed: 24203977]
19. Kaname T, Ki CS, Niikawa N, et al. Heterozygous mutations in cyclic AMP phosphodiesterase-4D (PDE4D) and protein kinase A (PKA) provide new insights into the molecular pathology of acrodysostosis. Cell Signal. 2014;26:2446–59. [PubMed: 25064455]
20. Elli FM, Bordogna P, de Sanctis L, et al. Screening of PRKAR1A and PDE4D in a large Italian series of patients clinically diagnosed with Albright hereditary osteodystrophy and/or pseudohypoparathyroidism. J Bone Miner Res. 2016;31:1215–24. [PubMed: 26763073]
21. Maass PG, Aydin A, Luft FC, et al. PDE3A mutations cause autosomal dominant hypertension with brachydactyly. Nat Genet. 2015;47: 647–53. [PubMed: 25961942]
22. Boda H, Uchida H, Takaiso N, et al. A PDE3A mutation in familial hypertension and brachydactyly syndrome. J Hum Genet. 2016;61 (8):701 −3. [PubMed: 27053290]
23. Ty JM, James MA. Failure of differentiation: part II (arthrogryposis, camptodactyly, clinodactyly, madelung deformity, trigger finger, and trigger thumb). Hand Clin. 2009;25:195–213. [PubMed: 19380060]
24. Williams SR, Aldred MA, Der Kaloustian VM, et al. Haploinsufficiency of HDAC4 causes brachydactyly mental retardation syndrome, with brachydactyly type E, developmental delays, and behavioral problems. Am J Hum Genet. 2010;87:219–28. [PubMed: 20691407]
25. Klopocki E, Hennig BP, Dathe K, et al. Deletion and point mutations of PTHLH cause brachydactyly type E. Am J Hum Genet. 2010;86:434–39. [PubMed: 20170896]
26. Maass PG, Wirth J, Aydin A, et al. A cis-regulatory sitedownregulates PTHLH in translocation t(8;12)(q13;p11.2) and leads to brachydactyly type E. Hum Mol Genet. 2010;19:848–60. [PubMed: 20015959]
27. Wang J, Wang Z, An Y, et al. Exome sequencing reveals a novel PTHLH mutation in a Chinese pedigree with brachydactyly type E and short stature. Clin Chim Acta. 2015;446:9–14. [PubMed: 25801215]
28. Thomas-Teinturier C, Pereda A, Garin I, et al. Report of two novel mutations in PTHLH associated with brachydactyly type E and literature review. Am J Med Genet A. 2016;170:734–42. [PubMed: 26640227]
29. Jamsheer A, Sowinska-Seidler A, Olech EM, et al. Variable expressivity of the phenotype in two families with brachydactyly type E, craniofacial dysmorphism, short stature and delayed bone age caused by novel heterozygous mutations in the PTHLH gene. J Hum Genet. 2016;61:457–61. [PubMed: 26763883]

30. Pereda A, Garzon-Lorenzo L, Garin I, et al. The p.R56* mutation in PTHLH causes variable brachydactyly type E. Am J Med Genet A. 2017;173:816–19. [PubMed: 28211986]

31. Bae J, Choi HS, Park SY, Lee DE, Lee S. Novel mutation in PTHLH related to brachydactyly type e2 initially confused with unclassical pseudopseudohypoparathyroidism. Endocrinol Metab (Seoul). 2018;33:252–59. [PubMed: 29947179]

32. Mannstadt M, Harris M, Bravenboer B, et al. Germline mutations affecting Galpha11 in hypoparathyroidism. N Engl J Med. 2013;368: 2532–34. [PubMed: 23802536]

33. Chillambhi S, Turan S, Hwang DY, Chen HC, Jüppner H,Bastepe M Deletion of the noncoding GNAS antisense transcript causes pseudohypoparathyroidism type Ib and biparental defects of GNAS methylation in cis. J Clin Endocrinol Metab. 2010;95: 3993–4002. [PubMed: 20444925]

34. Phelan MC, Rogers RC, Clarkson KB, et al. Albright hereditary osteodystrophy and del(2) (q37.3) in four unrelated individuals. Am J Med Genet. 1995;58:1–7. [PubMed: 7573148]

35. Long DN, McGuire S, Levine MA, Weinstein LS, Germain-Lee EL. Body mass index differences in pseudohypoparathyroidism type 1a versus pseudopseudohypoparathyroidism may implicate paternal imprinting of Galpha(s) in the development of human obesity. J Clin Endocrinol Metab. 2007;92:1073–79. [PubMed: 17164301]

36. Mouallem M, Shaharabany M, Weintrob N, et al. Cognitive impairment is prevalent in pseudohypoparathyroidism type Ia, but not in pseudopseudohypoparathyroidism: possible cerebral imprinting of Gsalpha. Clin Endocrinol (Oxf). 2008;68:233–39. [PubMed: 17803690]

37. Shoemaker AH, Jüppner H. Nonclassic features of pseudohypoparathyroidism type 1A. Curr Opin Endocrinol Diabetes Obes. 2017;24: 33–8. [PubMed: 27875418]

38. Maes C, Kronenberg HM. Bone development and remodeling In: Endocrinology. DeGroot LJ, Jameson JL, editors. Philadelphia, PA: WB Saunders; 2016 p. 1038–62.

39. Linglart A, Mahon MJ, Kerachian MA, et al. Coding GNAS mutations leading to hormone resistance impair in vitro agonist- and cholera toxin-induced adenosine cyclic 3', 5'-monophosphate formation mediated by human XLalphas. Endocrinology. 2006;147:2253–62. [PubMed: 16484323]

A

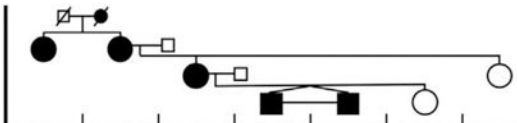

Code	190/II-1	190/II-2	190/III-1	190/IV-1	190/IV-2	190/IV-3	190/III-2
Birth weight (g)	3,000	2,400	3,200	1,680*	1,760*	4,210	3,350
Birth length (cm)	unknown	unknown	50.0	41.0	40.5	52.0	48.5
Adult height (cm)	151.0	155.0	160.0	169.5	172.5	168.0	164.0
z-score	-1.90	-1.30	-0.50	-0.90	-0.50	0.70	0.10
Adult weight (kg)	81	96	81	64	71	71	58
BMI (kg/m^2)	35.5	40.0	31.6	22.4	23.8	25.2	21.6
Short metacarpals/-tarsals	yes	yes	yes	yes	yes	no	no
Noted at what age	adult	6 yrs	unknown	2 yrs	2 yrs	n.a.	n.a
Delayed tooth eruption	no	no	1 molar missing	no	no	no	no
PTH (pg/ml; 15-65)	75.7	55.2	46.7	50.6	45.8	25.0	56.4
Calcium (mmol/L; 2.1-2.7)	2.34	2.43	2.43	2.46	2.42	2.42	2.35
Phosphate (mmol/L; 0.81-1.45)	1.18	1.10	1.14	1.21	1.07	0.92	1.25
25OHD (ng/ml; 20-50)	39.1	13.3	28.7	40.0	34.7	25.0	22.8
TSH (µU/ml; 0.27-4.2)	0.78	-	1.50	2.14	1.99	1.63	0.67
Variant at splice acceptor site of exon 3	yes	yes	yes	yes	yes	no	no
SNP rs6253	a/a	a/a	a/a	a/g	a/g	a/a	a/a

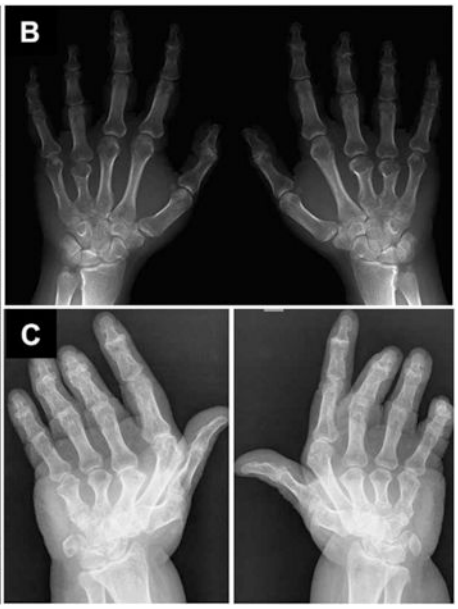

Fig. 1.

Pedigree of the investigated kindred and clinical, laboratory, and genetic findings. (*A*) Birth weights and lengths are provided, if known; adult height and weight measurements are also shown. Presence or absence of short metacarpal/metatarsals is indicated, along with the age at which these abnormalities were first noted. Laboratory results with units and adult normal ranges are provided, as well as the presence or absence of the identified variant at the splice acceptor site of *PTHLH* exon 3 and the genotype for SNP rs6253. Females = circles; males = squares; filled = affected; open = unaffected; small symbols = DNA not available;/ = deceased; * = born prematurely; n.a. = not applicable. (*B*,*C*) Hand radiographs of two affected family members, 190/III-1 and 190/II-1. Note shortening of the fourth or the third/fourth metacarpals, respectively, for the affected mother 190/III-1 and (B) shortening of multiple metacarpals as well as degenerative bone findings for the maternal aunt 190/II-1 (*C*).

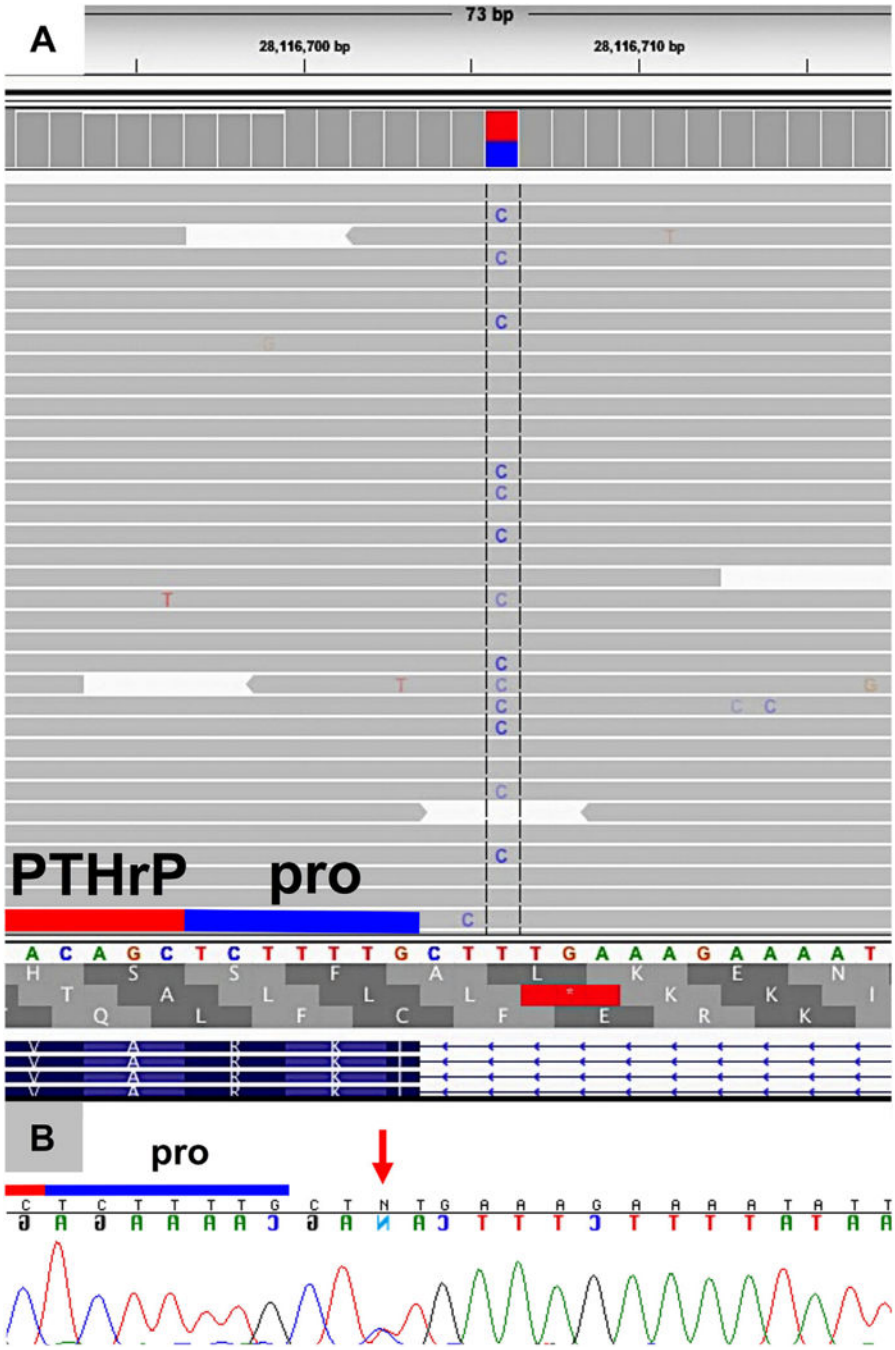

Fig. 2.

Identification of the putative mutation at the splice acceptor site of *PTHLH* exon 3. (*A*) Screen shot of the chromosome 12p region around the splice acceptor site at *PTHLH* exon 3 using the integrative genome viewer (IGV). Direction of transcription from right-to-left (as indicated by < at bottom of panel), thus showing the reverse nucleotide sequence. Note that T at position −3 is changed in approximately half of the sequence reads to C (A to G in sense direction). The last nucleotides encoding the prosequence of PTHrP and the beginning of the mature PTHrP are indicated by the horizontal blue and red bars, respectively. (*B*)

Direct nucleotide sequence analysis confirming in sense direction the A to G change (red arrow) that was identified by whole exome sequencing.

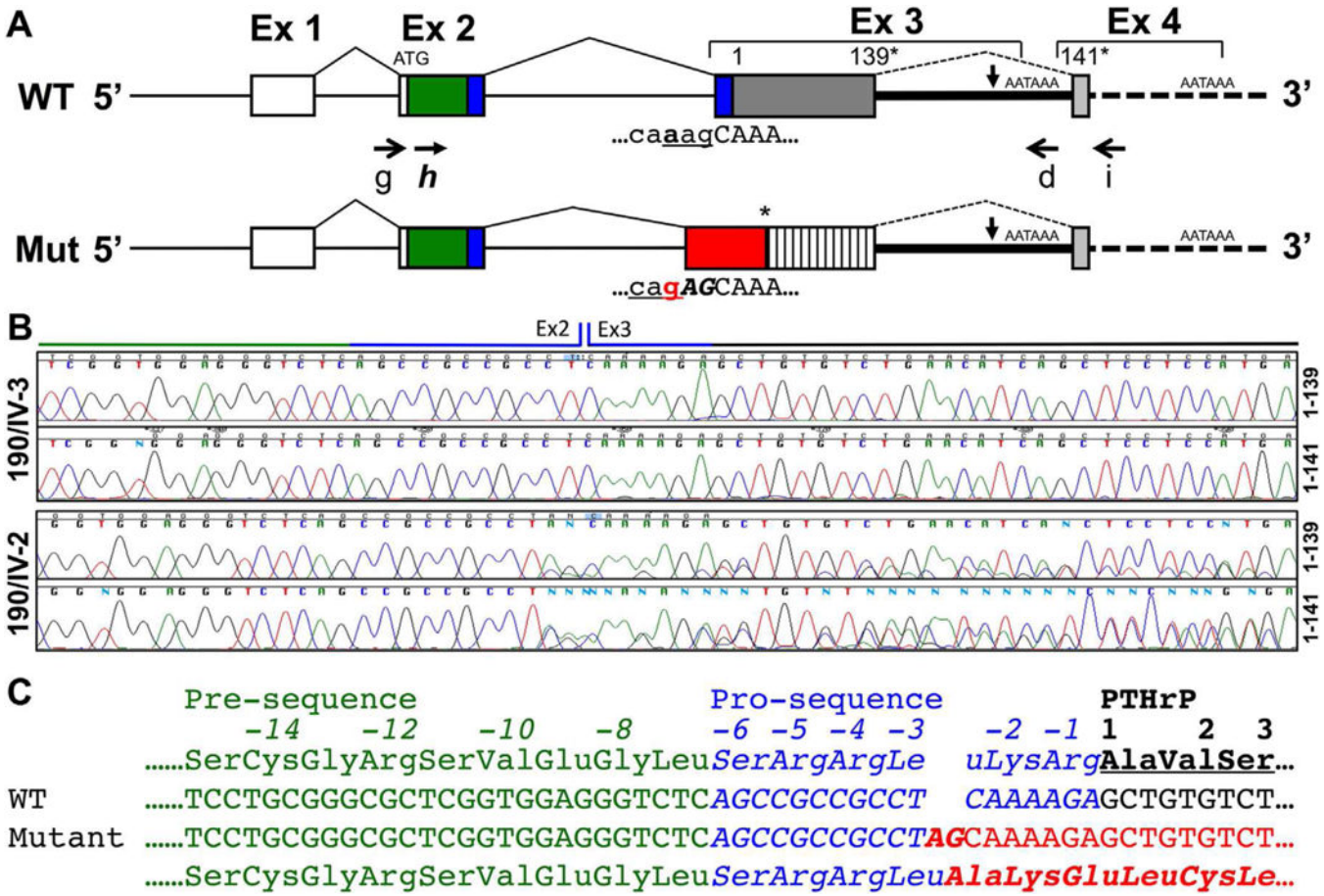

Fig. 3.

Amplification of cDNAs encoding PTHrP(1–139)or PTHrP(1–141) from an unaffected and an affected family member. (*A*) Schematic representation of WT and mutant (mut) *PTHLH*. GRCh37/hg19 was used for locations of coding and noncoding regions. Note that curation of this gene is not yet complete; hence, different nomenclatures have been used in the past for exon (Ex) numbering. WT allele: Ex 1 (chr12:28,122,958–28,123,200), noncoding (white); Ex 2 (chr12:28,122,327–28,122,443), noncoding portion (white), presequence, including the ATG (green) and portions of the prosequence of PTHrP (blue); Ex 3 (chr12:28,116,281–28,116,703 or 28,116,277–28,116,703), last two amino acid residues of the prosequence (blue) and the entire coding sequence of the PTHrP(1–139) variant (grey) followed by a termination codon (*), the 3'-noncoding region (thick black line) comprising SNP rs6253 (↓, 'a/g' polymorphism), and a polyadenylation signal (AATAAA); Ex 4 (chr12:28,111,492–28,111,501), amino acid residues 140 and 141 (light grey) of the alternatively spliced PTHrP (1–141) variant followed by a termination codon (*) and the 3'-noncoding region (thick dashed black line) comprising another polyadenylation signal (AATAAA); not shown is the exon giving rise to the PTHrP(1–173) splice variant, which is located between exons 3 and 4. Mutant (Mut) allele:Theadenine-to-guanine change (bold black and red letters) identified in genomic DNAof all affected family members at position −3 upstream of exon 3 generates a novel splice acceptor site (cag, instead of aag). This leads to a 5'-extension of exon 3 by two nucleotides and thus a change in the open-reading frame followed by an in-frame

termination codon (*) and novel 3'-noncoding sequence (white striped rectangle). The mRNA transcript derived from the mutant *PTHLH* allele comprises two additional nucleotides (bold italics) derived from genomic nucleotides at positions −2 and −1 up-stream of wild-type exon 3.(*B*) Nucleotide sequence of cDNAs derived from total RNA extracted from lymphoblastoid cells of 190/IV-3 (unaffected, upper sequences) or 190/IV-2 (affected, lower sequences). Portions of amplicons are shown that encode either PTHrP(1–139) (primers g and d) or PTHrP(1–141) (primers g and i); primer *h* was used for sequencing (see Fig. 1). Boundary between exon 2 (Ex 2) and exon 3 (Ex 3) is indicated; green, blue, and black lines above the sequences indicate portions of the mRNA that encode the presequence, the prosequence, and the secreted PTHrP, respectively. Indistinguishable results (nucleotide sequences not shown) were obtained also when using amplification primers e and d, or f and d (see also Supplementary Fig. 2). (*C*) WT nucleotide sequence using cDNA derived from the unaffected daughter 190/IV-3 and encoded amino acid sequence. Portions for the presequence (green), the prosequence (blue), and the secreted PTHrP (black, bold). Nucleotide sequence of the mutant cDNA derived from the affected son 190/IV-2 showing the insertion of two base pairs (red bold italics), resulting in a shift of the open-reading frame, thereby introducing 29 novel amino acid residues (*AKELCLNISSSMTRGSPSKIYGDDSSFTI**) followed by a termination codon; shown are the first of these novel residues that are unrelated to PTHrP (red, bold).